

A Symmetrical Quasi-Classical Spin-Mapping Model for the Electronic Degrees of Freedom in Non-Adiabatic Processes

Stephen J. Cotton and William H. Miller*

Department of Chemistry and Kenneth S. Pitzer Center for Theoretical Chemistry, University of California, Berkeley, Berkeley, California 94720, United States

Chemical Sciences Division, Lawrence Berkeley National Laboratory, Berkeley, California 94720, United States

ABSTRACT: A recent series of papers has shown that a symmetrical quasi-classical (SQC) windowing procedure applied to the Meyer–Miller (MM) classical vibronic Hamiltonian provides a very good treatment of electronically nonadiabatic processes in a variety of benchmark model systems, including systems that exhibit strong quantum coherence effects and some which other approximate approaches have difficulty in describing correctly. In this paper, a different classical electronic Hamiltonian for the treatment of electronically nonadiabatic processes is proposed (and “quantized” via the SQC windowing approach), which maps the dynamics of F coupled electronic states to a set of F spin- $1/2$ degrees of freedom (DOF), similar to the Fermionic spin model described by Miller and White (*J. Chem. Phys.* **1986**, *84*, 5059). It is noted that this spin-mapping (SM) Hamiltonian is an exact Hamiltonian if treated as a quantum mechanical (QM) operator—and thus QM’ly equivalent to the MM Hamiltonian—but that an analytically distinct classical analogue is obtained by replacing the QM spin-operators with their classical counterparts. Due to their analytic differences, a practical comparison is then made between the MM and SM Hamiltonians (when quantized with the SQC technique) by applying the latter to many of the same benchmark test problems successfully treated in our recent work with the SQC/MM model. We find that for every benchmark problem the MM model provides (slightly) better agreement with the correct quantum nonadiabatic transition probabilities than does the new SM model. This is despite the fact that one might expect, a priori, a more natural description of electronic state populations (occupied versus unoccupied) to be provided by DOF with only two states, i.e., spin- $1/2$ DOF, rather than by harmonic oscillator DOF which have an infinite manifold of states (though only two of these are ever occupied).

$$\begin{aligned}\hat{H}_{el} &= \sum_{i,j}^F \hat{S}_i^+ H_{ij} \hat{S}_j^- \\ &= \sum_{i,j}^F \left(\hat{S}_{x,i} \hat{S}_{x,j} + \hat{S}_{y,i} \hat{S}_{y,j} - i[\hat{S}_{x,i}, \hat{S}_{y,j}] \right) H_{ij} \\ &= \sum_i^F \left(\hat{S}_{x,i}^2 + \hat{S}_{y,i}^2 + \hat{S}_{z,i} \right) H_{ii} \\ &\quad + 2 \sum_{i<j}^F \left(\hat{S}_{x,i} \hat{S}_{x,j} + \hat{S}_{y,i} \hat{S}_{y,j} \right) H_{ij},\end{aligned}$$

1. INTRODUCTION

In a series of recent papers,^{1–4} we have described and evaluated a symmetrical quasi-classical (SQC) procedure for extracting approximate quantum state information for selected degrees of freedom (DOF) within the general framework of classical molecular dynamics (MD) simulation. The first paper¹ (paper I) presented the basic SQC approach and applied it to reactive $H + H_2 \rightarrow H_2 + H$ (collinear) scattering calculations in order to “quantize” the vibrational DOF of the diatom and thereby obtain approximate vibrational quantum state-to-state information. The two papers which followed^{2,3} (papers II and III) applied the SQC approach to the much more interesting and challenging problem of treating electronically nonadiabatic phenomena. This was done by applying the SQC-quantization procedure to excitations in the electronic oscillator DOF of the classical Meyer–Miller (MM) Hamiltonian,⁵ the excitations representing the occupations of the various electronic states. It was found that this very simple, purely classical approach provides a very good description of nonadiabatic effects for a suite of standard benchmark model problems for which exact quantum results are available for comparison, including systems exhibiting strong quantum coherence effects, systems repre-

sentative of condensed-phase nonadiabatic dynamics, and some which other simple approaches have difficulty in describing correctly (e.g., the asymmetric spin-boson problem (see paper II) and the inverted regime⁶ in electron transfer processes (see paper III)).

The basic idea behind the SQC methodology is quite simple: the relevant DOF are “quantized” within the context of classical trajectory simulation by applying a “window function” symmetrically (i.e., initially and finally) to the classical action variables associated with the DOF of interest. As explained in paper I with respect to reactive scattering and vibrational quantization, this results in a smoothing of the singularities appearing in classical S-matrix theory.⁷ Assuming that one chooses the window functions to be simple histograms (i.e., “boxes”, though this is not necessary), the SQC model may also be thought of as a modification of the original⁸ quasi-classical

Special Issue: Dynamics of Molecular Collisions XXV: Fifty Years of Chemical Reaction Dynamics

Received: June 20, 2015

Revised: August 14, 2015

Published: August 24, 2015

(QC) model, with two key variations. The first of these is the “symmetrical” aspect,⁹ i.e., that the initial classical actions are sampled from histograms centered about the initial quantum (integer) values of the actions, analogous to how the final classical actions are “collected” in histograms centered about the possible final quantum (integer) values (to determine the probability of reaching each possible final quantum state). This symmetrical treatment insures time-reversal symmetry—that the forward and backward transition probabilities are equal (as they rigorously should be)—something not true of the original QC treatment.

The second variation from the original QC model is that the window functions are given a reduced (fractional) width instead of being of unit width (as in the original QC model). This second variation was motivated by the work of Bonnet and Rayez¹⁰ who used narrowed Gaussian window functions to constrain molecular vibrations about the quantum values (though not done so symmetrically). As noted previously,¹ in our experience, histogram and Gaussian window functions of comparable width yield very similar results; thus, for our purposes, the key aspect of Bonnet and Rayez’s work is that they took advantage of narrowed window functions (even if not applied symmetrically). Related to this, in our modeling of nonadiabatic processes through SQC-quantization of the MM Hamiltonian, we have in all calculations tied the width of the electronic action window functions to the amount of zero-point energy (ZPE) initially present in each electronic oscillator; thus, our use of narrowed window functions also bears a relationship to Stock’s work^{11,12} that found better results with the QC treatment of the MM Hamiltonian if less than the full quantum ZPE was included. The linking of the window function width to the fraction of quantum ZPE also makes the SQC/MM model fully specified by a single parameter.

As previously emphasized, the MM Hamiltonian provides a consistent framework for treating the coupled dynamics of the electronic and nuclear DOF by treating all the DOF on an equal footing. This is true whether the MM Hamiltonian is treated as a QM operator (whereby it is exactly equivalent to the coupled-channel Schrödinger equation), treated via a uniform semiclassical (SC) approximation such as the SC initial value representation (IVR),^{13,14} or treated completely classically (as done in our SQC work); the key point is that at each level of approximation the electronic and nuclear DOF are treated equivalently, so that the dynamic interactions between the different classes of DOF are properly incorporated.

Finally, there is one further point about the classical SQC/MM approach that we would like to emphasize, namely (as pointed out in the original MM paper), that when treated classically the MM Hamiltonian generates what are essentially “Ehrenfest trajectories”; i.e., the nuclear DOF evolve on an effective potential energy surface (PES) which is an instantaneous weighted average over all the (fractionally) occupied electronic states. This has thus often led to the conclusion that MM-based approaches are the “Ehrenfest method”, but this is not the case. It *would* be the Ehrenfest method if there were no zero point energy (ZPE) in the electronic oscillators of the initially unoccupied electronic states, for in this case there would be only one set of initial conditions for the electronic DOF, and thus only one trajectory (for given initial conditions of the nuclear DOF), leading to the well-known unphysical result of ending up on an average PES. With ZPE in all the electronic oscillators, however, there is an ensemble of trajectories, and the SQC approach determines the

population of each electronic state as the fraction of this ensemble for which the time-evolved electronic actions fall within a window about the integer (quantum) actions for that state, i.e., the fraction that are on the PES (within a “window”) for that state. Different final electronic states thus involve different classical trajectories. Therefore, even though the equations of motion are Ehrenfest, the initial conditions of the electronic variables are not Ehrenfest, nor is the way the final electronic action variables are “processed” to obtain the probabilities of being in various electronic states.

Although the SQC/MM approach has given quite good results for the examples treated to date,^{2,3} the purpose of this paper is to point out that the MM mapping of electronic states onto (harmonic) oscillators is not the only possible mapping one could use, and in some ways, it is not the most natural one; i.e., a harmonic oscillator has an infinite number of energy levels, even though only levels 0 and 1 are involved in the nonadiabatic dynamics (since the sum of the electronic quantum numbers/action variables is 1, and this quantity is conserved by the dynamics). A more natural mapping would thus seem to be onto DOF that have only two quantum states, i.e., a spin- $1/2$ DOF for each electronic state (spin-up representing the state being occupied and spin-down the state unoccupied). This is essentially what Miller and White¹⁵ did in obtaining a classical model for each Fermionic DOF of the many electron Hamiltonian, but it has never (to our knowledge) been explored for mapping electronic states. The purpose of this paper is thus to define and explore this spin mapping of electronic states, e.g., seeing how it compares to the MM oscillator mapping both formally and also how it handles a standard suite of model problems (for which the SQC/MM model performs quite well).

The organization of this paper is as follows: [Section 2](#) presents the new SQC spin-mapping (SM) model, its derivation as an exact Hamiltonian operator, its relationship to the MM Hamiltonian, and its implementation within the SQC framework. [Section 3](#) presents results for the application of this new approach to the core benchmarks used to evaluate the previous SQC/MM approach.

We emphasize that, although both the Meyer–Miller (MM) and spin-mapping (SM) vibronic Hamiltonians are exact when treated as QM operators, all the calculations presented in this paper treat them classically, as they would be implemented within the context of purely classical MD simulation. Our conclusions are presented in [section 4](#).

2. A SPIN-MAPPING (SM) HAMILTONIAN FOR THE TREATMENT OF ELECTRONICALLY NON-ADIABATIC PROCESSES

2.1. Basic Derivation. To derive the new spin-mapping (SM) model and see its relationship to the Meyer–Miller (MM) model, we begin with a generic representation of a Hamiltonian operator for F electronic states which may be written in second-quantization as

$$\hat{H}_{\text{el}}(\hat{\mathbf{R}}) = \sum_{i,j}^F \hat{a}_i^\dagger H_{ij}(\hat{\mathbf{R}}) \hat{a}_j \quad (1)$$

where \hat{a}_i^\dagger and \hat{a}_j are the creation and annihilation (ladder) operators corresponding to the i th and j th electronic states, respectively. This Hamiltonian is of course an exact representation in the relevant subspace of single excitations

(here, an excitation represents the occupation of the corresponding electronic state), as may be verified by forming matrix elements of \hat{H}_{el} in the basis of single excitations:

$$|i\rangle = \underbrace{|0, \dots, n_i = 1, \dots, 0\rangle}_{F\text{-states}}$$

Though different from Meyer and Miller's original heuristic procedure, the most rigorous way to derive¹⁶ the MM Hamiltonian is via "Schwinger bosonization", i.e., to take the underlying DOF in eq 1 to be harmonic oscillators (bosons) of unit mass and frequency, whereby the ladder operators can be expressed in terms of coordinate and momentum operators as

$$\hat{a}_i = \frac{1}{\sqrt{2}}(\hat{x}_i + i\hat{p}_i) \quad (2a)$$

$$\hat{a}_i^\dagger = \frac{1}{\sqrt{2}}(\hat{x}_i - i\hat{p}_i) \quad (2b)$$

Substituting these into eq 1 gives

$$\begin{aligned} \hat{H}_{\text{el}} &= \sum_{i,j}^F \hat{a}_i^\dagger \hat{a}_j H_{ij} \\ &= \sum_{i,j}^F \frac{1}{2}(\hat{p}_i \hat{p}_j + \hat{x}_i \hat{x}_j - i[\hat{p}_i, \hat{x}_j])H_{ij} \\ &= \sum_i^F \left(\frac{1}{2}\hat{p}_i^2 + \frac{1}{2}\hat{x}_i^2 - \frac{1}{2} \right) H_{ii} + \sum_{i<j}^F (\hat{p}_i \hat{p}_j + \hat{x}_i \hat{x}_j) H_{ij} \end{aligned} \quad (3)$$

Note that the $[\hat{p}, \hat{x}]$ commutator is related to how ZPE is treated in the diagonal elements (it is zero in the off-diagonal, since \hat{p}_i and \hat{x}_j commute for $i \neq j$); note that no approximation is made in arriving at eq 3.

The classical electronic Hamiltonian of MM is thus obtained by taking eq 3 to be a classical Hamiltonian, replacing all quantum operators (nuclear and electronic) with their classical counterparts. Additionally, in our recent SQC work, we have incorporated a ZPE γ -parameter (in the diagonal elements of eq 3) and chosen it to be less than the quantum value of $1/2$. Including the classical nuclear kinetic energy term gives the complete classical vibronic Hamiltonian for F electronic states as

$$\begin{aligned} H(\mathbf{P}, \mathbf{R}, \mathbf{p}, \mathbf{x}) &= \frac{|\mathbf{P}|^2}{2\mu} + \sum_i^F \left(\frac{1}{2}p_i^2 + \frac{1}{2}x_i^2 - \gamma \right) H_{ii}(\mathbf{R}) \\ &\quad + \sum_{i<j}^F (p_i p_j + x_i x_j) H_{ij}(\mathbf{R}) \end{aligned} \quad (4)$$

from which classical trajectories are computed via Hamilton's equations, i.e., classical molecular dynamics (MD) for nuclear and electronic DOF. The electronic DOF are "quantized" within the SQC framework (as described in section 1 and the Appendix) to obtain the probabilities for transitions between specific initial and final electronic states. Setting $\gamma = 1/2$ in eq 4 recovers Meyer and Miller's original version.

The MM Hamiltonian may also be expressed in terms of harmonic oscillator action-angle variables $\{n_i, q_i\}$ using the canonical transformation

$$x_i = \sqrt{2(n_i + \gamma)} \cos(q_i) \quad (5a)$$

$$p_i = -\sqrt{2(n_i + \gamma)} \sin(q_i) \quad (5b)$$

whose inverse is

$$n_i = \frac{1}{2}p_i^2 + \frac{1}{2}x_i^2 - \gamma \quad (6a)$$

$$q_i = -\tan^{-1}\left(\frac{p_i}{x_i}\right) \quad (6b)$$

Using these expressions to transform eq 4 yields

$$\begin{aligned} H(\mathbf{P}, \mathbf{R}, \mathbf{p}, \mathbf{x}) &= \frac{|\mathbf{P}|^2}{2\mu} + \sum_i^F n_i H_{ii}(\mathbf{R}) \\ &\quad + 2 \sum_{i<j}^F \sqrt{n_i + \gamma} \sqrt{n_j + \gamma} \cos(q_i - q_j) H_{ij}(\mathbf{R}) \end{aligned} \quad (7)$$

The diagonal terms in eq 7 show that the actions $\{n_i\}$ represent the occupations of the F electronic states—which are what are "windowed" within the SQC framework (i.e., the n_i 's are sampled initially and binned finally from window functions centered at the quantum (integer) values of the actions (0 or 1)). Trajectory calculations, however, are typically carried out (and are here) in the Cartesian representation of eq 4. (This is because the equations of motion generated from the Cartesian MM Hamiltonian are free from the singularities and transcendental functions present in equations of motion generated from eq 7.)

2.2. The Spin-Mapping (SM) Hamiltonian. As described in section 1, recent use of the Cartesian MM Hamiltonian within the SQC framework has proved quite successful, but it is not the only way of using the generic Hamiltonian of eq 1 to obtain a classical model for the electronic DOF. That is, it is not necessary to choose the underlying DOF for the creation–annihilation operators to be harmonic oscillators, and in some ways, this choice does not seem the most natural one, since a harmonic oscillator has an infinite number of quantum states (even though only states 0 and 1 are ever occupied and have any physical significance). Different choices for the underlying DOF will lead to different Hamiltonians, equivalent QM'ly but (possibly) not equivalent in their classical analogue. Thus, although the MM Hamiltonian has been seen to work quite well (particularly when implemented within the SQC framework), it is useful to explore whether a different choice for \hat{a}^\dagger and \hat{a} in eq 1 may perform even better.

Since only two states (occupied or unoccupied) for each DOF in eq 1 are ever utilized, a natural choice for each underlying DOF would seem to be that which has only two quantum states, i.e., a spin- $1/2$, for which the creation–annihilation operators are the usual angular momentum ladder operators:

$$\hat{S}_i^+ = \hat{S}_{x,i} + i\hat{S}_{y,i} \quad (8a)$$

$$\hat{S}_i^- = \hat{S}_{x,i} - i\hat{S}_{y,i} \quad (8b)$$

Here the two states per DOF are $S_{z,i} = +1/2$ (spin-up) for state $|i\rangle$ occupied and $S_{z,i} = -1/2$ (spin-down) for state $|i\rangle$ unoccupied, rather than an infinite manifold of vibrational states for each electronic DOF which are theoretically present

but only two of which (the ground and first excited states) have any physical significance.

We thus obtain the “spin-mapping” (SM) Hamiltonian in analogy with the derivation of eq 3 by using eq 8 as the ladder operators in eq 1. This gives

$$\begin{aligned}\hat{H}_{\text{el}} &= \sum_{i,j}^F \hat{S}_i^+ H_{ij} \hat{S}_j^- \\ &= \sum_{i,j}^F (\hat{S}_{x,i} \hat{S}_{x,j} + \hat{S}_{y,i} \hat{S}_{y,j} - i[\hat{S}_{x,i}, \hat{S}_{y,j}]) H_{ij} \\ &= \sum_i^F (\hat{S}_{x,i}^2 + \hat{S}_{y,i}^2 + \hat{S}_{z,i}) H_{ii} + 2 \sum_{i<j}^F (\hat{S}_{x,i} \hat{S}_{x,j} + \hat{S}_{y,i} \hat{S}_{y,j}) H_{ij}\end{aligned}\quad (9)$$

where in the last step the angular-momentum commutator, $[\hat{S}_x, \hat{S}_y] = i\hat{S}_z$, has been used (and, as in eq 3, the commutator is zero between different DOFs). An equivalent expression with diagonal terms depending solely on $\{\hat{S}_{z,i}\}$ is obtained by using

$$\hat{S}_x^2 + \hat{S}_y^2 = \hat{S}^2 - \hat{S}_z^2$$

which can be further simplified by noting that the diagonal values of S_z are $\{\pm 1/2\}$, so that

$$S^2 - S_z^2 = \frac{1}{2} \left(\frac{1}{2} + 1 \right) - \left(\pm \frac{1}{2} \right)^2 = \frac{1}{2}$$

Equation 9 then becomes

$$\hat{H}_{\text{el}} = \sum_i^F \left(\hat{S}_{z,i} + \frac{1}{2} \right) H_{ii} + 2 \sum_{i<j}^F (\hat{S}_{x,i} \hat{S}_{x,j} + \hat{S}_{y,i} \hat{S}_{y,j}) H_{ij}\quad (10)$$

which we emphasize (once the nuclear kinetic energy operator is added) constitutes an exact quantum representation of any coupled nuclear-electronic system with (real, symmetric) diabatic matrix elements $\{H_{ij}(\mathbf{R})\}$, just as eq 3 shows the same for the MM Hamiltonian. However, despite their equivalence when treated QM'ly, these Hamiltonians do not have the same algebraic form, and while this does not affect their exactness QM'ly, it *does* make a difference when they are treated classically.

Just as for the classical MM Hamiltonian, the classical analogue of the quantum SM Hamiltonian of eq 10 is obtained by replacing the quantum spin operators by their classical angular-momenta counterparts. A comparison of the two classical Hamiltonians is most revealing when both are expressed in their action-angle variables. Equation 7 gives this for the MM Hamiltonian, and for the classical SM Hamiltonian, one uses the following expression for classical angular momenta in terms of their action-angle variables $\{m_\nu, q_\nu\}$

$$\vec{S}_i \equiv \begin{bmatrix} S_{x,i} \\ S_{y,i} \\ S_{z,i} \end{bmatrix} = \begin{bmatrix} \sqrt{S^2 - m_i^2} \cos(q_i) \\ \sqrt{S^2 - m_i^2} \sin(q_i) \\ m_i \end{bmatrix}\quad (11)$$

To correspond more closely to the MM Hamiltonian, one may express the angular momentum action variables $\{m_i\}$ in terms of the MM action variables, $n_i \equiv m_i + 1/2$, which have quantum values $n_i \in \{0, 1\}$. With the relation between S^2 and the MM

parameter γ , $S^2 = (\gamma + 1/2)^2$, the classical SM Hamiltonian corresponding to eq 10 is (with the addition of the nuclear kinetic energy)

$$\begin{aligned}H(\mathbf{P}, \mathbf{R}, \mathbf{n}, \mathbf{q}) &= \frac{|\mathbf{P}|^2}{2\mu} + \sum_i^F n_i H_{ii}(\mathbf{R}) \\ &+ 2 \sum_{i<j}^F \sqrt{(n_i + \gamma)(1 + \gamma - n_i)} \\ &\times \sqrt{(n_j + \gamma)(1 + \gamma - n_j)} \\ &\times \cos(q_i - q_j) H_{ij}(\mathbf{R})\end{aligned}\quad (12)$$

which is the form to be compared with the action-angle version of the MM Hamiltonian of eq 7: one sees that the diagonal terms are identical; in the off-diagonal terms, the factors $\sqrt{n_i + \gamma}$ for each electronic DOF are the same for the two, but the SM Hamiltonian contains the additional factor $\sqrt{1 + \gamma - n_i}$ for each electronic DOF. The factor $\sqrt{n_i + \gamma}$ insures that $n_i(t)$ never falls below $-\gamma$ for any time t , and similarly, the factor $\sqrt{1 + \gamma - n_i}$ insures that it never exceeds $1 + \gamma$; i.e., in combination, the two factors ensure that $n(t)$ remains in the interval $[-\gamma, 1 + \gamma]$ for all t , which is of course the classical counterpart of the SM Hamiltonian representing a system of only two quantum states. In contrast, the MM Hamiltonian only requires that $n(t) > -\gamma$ for all time, which is consistent with its DOF being harmonic oscillators (though one should note that, because the MM Hamiltonian conserves the total action, $\sum_i^F n_\nu$, there is an upper limit on each n_i which results from the system's total initial action).

It is also instructive to compare the present SM model with the earlier spin-matrix mapping (SMM) model of Meyer and Miller.¹⁷ This prior model was also based on the notion of using a classical spin-representation for electronic DOF; however, the SMM model used a *single* spin DOF to represent all the electronic occupations: one spin- $1/2$ DOF ($m \in \{+1/2, -1/2\}$) to represent two electronic states, one spin-1 DOF ($m \in \{+1, 0, -1\}$) to represent three electronic states, and so forth. (For two electronic DOFs, this was shown to be equivalent to the MM model (provided one sets $n_1 \rightarrow n$ and $n_2 \rightarrow 1 - n$ in the MM model), but it is not equivalent to the MM model for three or more electronic states.) In contrast, in the SM model presented here, however many electronic states there are, each is represented by its own spin- $1/2$ DOF (equal, QM'ly, to $+1/2$ for occupied and $-1/2$ for unoccupied), and (as shown) the model is analytically distinct from the MM model for any number of electronic states.

In summary, though the MM and SM Hamiltonians have many similarities in their algebraic structure—and are completely equivalent when implemented fully QM'ly—they are not the same classically, and they embody physically different ways of representing the electronic DOF. Whether or not these differences in algebraic form lead to significant differences in results for various practical problems (calculated using the SQC protocol) will be explored below.

2.3. Implementation Details and Practical Modifications. As with the classical MM Hamiltonian, trajectories may be generated with the SM Hamiltonian in terms of action-angle variables, i.e., in terms of $\{m_\nu, q_\nu\}$ using eq 12; however (as with the MM model), it is preferable to do the dynamics directly in a Cartesian representation, $\{S_{x,\nu}, S_{y,\nu}, S_{z,\nu}\}$, where, as with the MM

model, the equations of motion are free from singularities and transcendental function evaluations. This has been done using the following vector equation of motion for the Cartesian spin components

$$\frac{d\vec{S}_i}{dt} = \frac{\partial H_{el}(\mathbf{R}, \vec{S}_i)}{\partial \vec{S}_i} \times \vec{S}_i \quad (13)$$

which is equivalent to applying Hamilton's equations in terms of $\{m_i, q_i\}$ to eq 10 after substituting eq 11 for each spin DOF (as one can verify with the chain rule). Hamilton's equations are then integrated in the usual manner to determine the trajectories for the nuclear DOF (\mathbf{P}, \mathbf{R}) (while simultaneously integrating eq 13).

Although it is preferable to run trajectories in terms of $\{\vec{S}_i\}$, the electronic DOF must still be sampled initially and binned finally (within the SQC framework) in terms of the action-angle variables $\{m_i, q_i\}$, as given in eq 11. This is, of course, required because the actions $\{m_i\}$ are the classical analogues of the angular momentum projection quantum numbers, and eq 11 illustrates again that $S_{z,i}$ indicates the occupation of electronic state $|i\rangle$. Equation 11 is thus used to set the initial conditions of $\{\vec{S}_i\}$ after choosing the actions $\{m_i\}$ uniformly within a distance γ of the quantum half-integer values of $\pm 1/2$ and choosing the conjugate angles $\{q_i\}$ uniformly between 0 and 2π . Note that eq 11 is not needed for binning the final actions, since the final values of $\{S_{x,i}\}$ and $\{S_{y,i}\}$ are not used (and $S_z = m$).

As before,¹⁸ it is also useful to add and subtract the average of the diagonal elements of the classical electronic Hamiltonian, which has the effect that the diagonal terms in eq 10, $\sum_i^F (S_{z,i} + 1/2)H_{ii}$ can be expressed in the more symmetrical form

$$\bar{H} + \frac{1}{F} \sum_{i < j}^F (S_{z,i} - S_{z,j}) \cdot (H_{ii} - H_{jj}) \quad (14)$$

where $\bar{H} \equiv (1/F) \sum_i^F H_{ii}$. Doing this and adding the classical nuclear kinetic energy term gives the final form of the classical vibronic SM Hamiltonian

$$H(\mathbf{P}, \mathbf{R}, \{\vec{S}_i\}) = \frac{|\mathbf{P}|^2}{2\mu} + \bar{H}(\mathbf{R}) + \frac{1}{F} \sum_{i < j}^F (S_{z,i} - S_{z,j}) \times (H_{ii}(\mathbf{R}) - H_{jj}(\mathbf{R})) + 2 \sum_{i < j}^F (S_{x,i}S_{x,j} + S_{y,i}S_{y,j}) \cdot H_{ij}(\mathbf{R}) \quad (15)$$

which is used in all the calculations below. (A similarly transformed version of the MM Hamiltonian (as detailed in paper II) has also been used in the calculations below.) Note that if this SM Hamiltonian is treated as a QM operator, it is still exact because it generates the correct matrix elements (the same as eq 10). Symmetrical quantization within the SQC/SM model proceeds analogously to how it is done in the SQC/MM model, as outlined in the Appendix, including renormalizing the final binned probabilities using eq 28.

Finally, there is the choice of S^2 for use in eq 11 and the selection of the ZPE γ -parameter. Consistent with the discussion in section 2.2 (and also with the justification in the Appendix of paper II), we take the quantum value for $S^2 = 3/4$, and with the relation between S^2 and γ , i.e., $S^2 = (1/2 + \gamma)^2$,

this leads to $\gamma = (\sqrt{3} - 1)/2 \approx 0.366$ that we have found to be nearly optimal in all previous calculations with the MM model. The SQC procedure thus uses a "window" of $\pm\gamma$ about the quantum values of $m = S_z = \pm 1/2$. Other values of S^2 and γ have been considered for the present SM model, but the values noted here are nearly optimal in all examples.

3. BENCHMARK RESULTS COMPARING THE SQC/SM AND SQC/MM APPROACHES

A suite of benchmark electronically nonadiabatic model problems were previously used to evaluate the SQC/MM approach (see paper II). Here the new SQC/SM approach is applied to (the most important of) the same test problems so that it may be similarly evaluated—and also so that it may be directly compared to the SQC/MM approach (previously seen to provide an excellent treatment of these problems). In all cases, the SQC protocol was used to "quantize" the initial and final electronic action variables for the MM and SM classical vibronic Hamiltonian models.

3.1. Single and Dual Avoided Crossings. The first benchmarks to which the SM model is applied are the single and dual avoided crossing problems originally used by Tully¹⁹ to test the fewest-switches surface hopping approach. Both are one-dimensional scattering problems: the system is initialized on one electronic potential energy surface (PES) far from the region of nonadiabatic coupling but given some initial inbound momentum, resulting in the electronically nonadiabatic interaction and four possible outcomes: reflection or transmission on either the upper or lower surfaces.

The single avoided crossing problem is given by the following diabatic Hamiltonian matrix elements

$$H_{11}(R) = \begin{cases} A(1 - e^{-BR}) & R \geq 0 \\ -A(1 - e^{BR}) & R < 0 \end{cases} \\ H_{22}(R) = -H_{11}(R) \\ H_{12}(R) = Ce^{-DR^2} \quad (16)$$

where $A = 0.01$, $B = 1.6$, $C = 0.005$, and $D = 1$ (all expressed in atomic units).

Likewise, the dual avoided crossing problem is given by

$$H_{11}(R) = 0 \\ H_{22}(R) = -Ae^{-Bx^2} + E_0 \\ H_{12}(R) = Ce^{-DR^2} \quad (17)$$

where $A = 0.1$, $B = 0.28$, $C = 0.015$, $D = 0.06$, and $E_0 = 0.05$. For both test problems, the mass associated with nuclear coordinate R is typically (and here) taken to be 2000 (in atomic units). Further details may be found in paper II.²

Results for the single avoided crossing problem are shown in Figure 1 along with the exact quantum result. The displayed results correspond to the probability of transmission through the region of nonadiabatic coupling and ending up on the lower surface, $T_{2 \leftarrow 1}$. (Because the surfaces cross, switching from diabatic surface H_{11} to H_{22} corresponds to remaining on the lower adiabatic surface.)

It is seen that the MM and SM models both are in reasonably good agreement with the correct quantum result, though the

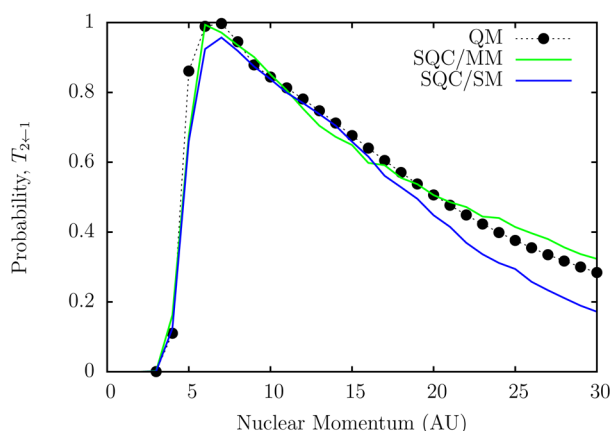


Figure 1. Single avoided crossing problem.

MM model is somewhat better, particularly in the high-momentum region where the SM result falls off too rapidly.

Figure 2 shows analogous lower surface transmission, $T_{1 \leftarrow 1}$, results for the dual avoided crossing problem. (Here there are

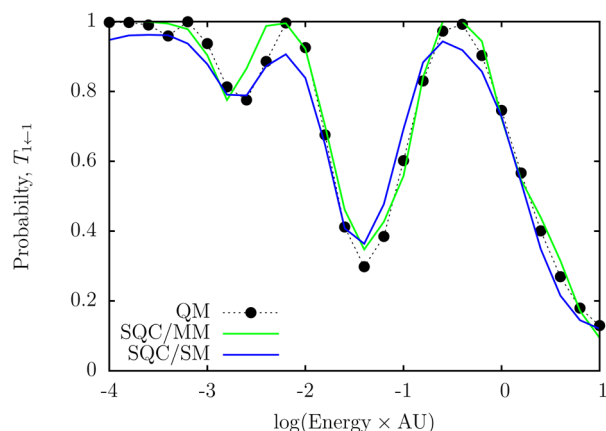


Figure 2. Dual avoided crossing problem.

two crossings, so $T_{1 \leftarrow 1}$ corresponds to ending up on the lower surface.) Here too one sees that both the MM and SM models are in reasonably good agreement with the quantum results, e.g., both giving a good description of oscillatory behavior in the energy dependence of the transition probability (“Stückelberg oscillations”), a quantum coherence effect due to the possibility of the transition between surfaces taking place in either of the crossing regions. Again, though, the results of the MM model are seen to be slightly better than those of the SM model.

For these two examples, therefore, the MM and SM classical electronic Hamiltonians are seen to give similar results, though the former seems to provide a slightly superior description.

3.2. The Spin-Boson Problem. The second set of benchmarks consists of different versions of the well-studied “spin-boson” problem. As detailed in paper II, this problem models dissipative electronically nonadiabatic processes in the condensed phase with a pair of offset multidimensional harmonic oscillators energetically biased by 2ϵ , and coupled together by nonadiabatic coupling constant Δ (which is independent of nuclear coordinates $\{Q_k\}$):

$$H_{11}(\mathbf{Q}) = \sum_{k=1}^G \frac{1}{2} \omega_k^2 Q_k^2 + \sum_{k=1}^G c_k Q_k + \epsilon$$

$$H_{22}(\mathbf{Q}) = \sum_{k=1}^G \frac{1}{2} \omega_k^2 Q_k^2 - \sum_{k=1}^G c_k Q_k - \epsilon$$

$$H_{12}(\mathbf{Q}) = H_{21}(\mathbf{Q}) = \Delta \quad (18)$$

Setting $\epsilon = 0$ gives the symmetric version of the problem; $\epsilon \neq 0$ gives the asymmetric version (which is typically much more challenging for any approximate treatment). “Quantum coherence” is seen when the temperature is low (or equivalently the electronic coupling Δ is small), as determined by selecting an appropriate thermal distribution for the initial oscillator coordinates $\{Q_k\}$ and momenta $\{P_k\}$

$$\rho(\mathbf{P}, \mathbf{Q}) \propto \prod_{k=1}^G e^{-\alpha_k [(1/2)P_k^2 + (1/2)\omega_k^2(Q_k + (c_k/\omega_k)^2)]} \quad (19)$$

where $\alpha_k = (2/\omega_k) \tanh(\beta\omega_k/2)$.

The frequencies $\{\omega_k\}$ in eq 18 are chosen according to some spectral density function

$$J(\omega) = \frac{\pi}{2} \sum_{k=1}^G \frac{c_k^2}{\omega_k} \delta(\omega - \omega_k) \quad (20)$$

characteristic of a specific condensed phase environment (such as a particular solvent’s distribution of vibrational frequencies). As in paper II, the discrete frequencies are selected from a continuous “Ohmic” spectral density function

$$J(\omega) = \eta \omega e^{-\omega/\omega_c} \quad (21)$$

having characteristic frequency ω_c and coupling (or friction) parameter η . The coupling constants $\{c_k\}$ appearing in eq 18 are then given (from eqs 20 and 21) by

$$c_k = \sqrt{(2/\pi) \Delta \omega \omega_k J(\omega_k)} \quad (22)$$

Results for the symmetric spin-boson problem, at high and low temperatures, are shown in parts a and b of Figure 3, respectively (with various parameters as given in the figure captions). Specifically, the results correspond to the time-dependent population difference between electronic states 1 and 2

$$D(t) = P_{1 \leftarrow 1}(t) - P_{2 \leftarrow 1}(t)$$

after the system is initialized in electronic state 1 with the appropriate thermal distribution for the nuclear DOF (as given in eq 19). Results calculated using both the MM and SM models are plotted along with the exact quantum results.²⁰

Likewise, parts a and b of Figure 4 show analogous results (versus benchmark quantum calculations²¹) for the asymmetric problem at high and low temperatures (and again with various parameters as given in the figure captions). All the SQC calculations employed 100 modes, i.e., $G = 100$ in eq 18, so of a dimensionality on the order of what would be relevant to an electronic transition in the condensed phase.

As with the single and dual avoided crossing problems, for the spin-boson problem, the MM and SM models (implemented within the SQC framework) are seen to give roughly comparable results over the four parameter regimes tested, with the MM model generally being slightly superior. The one exception is the symmetric version of the spin-boson problem

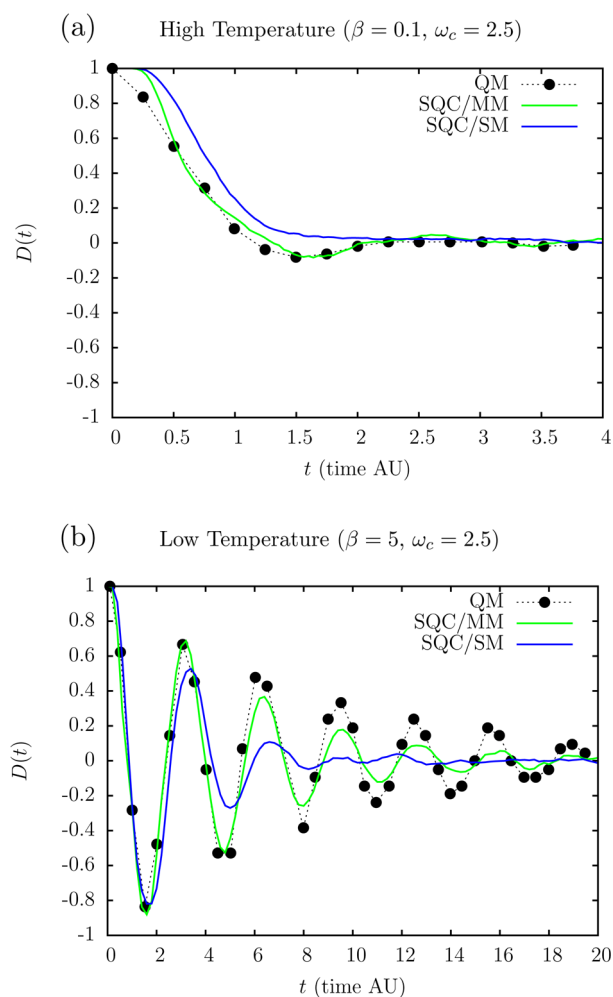


Figure 3. Symmetric spin-Boson problem ($\epsilon = 0$, $\alpha = 0.09$, $\Delta = 1$).

at low temperature, where the MM model is seen to perform much better—the coherence structure calculated with the SM model is seen to decay much too rapidly. The results are thus consistent with the other examples: while the SM model does provide reasonable results over this suite of test benchmarks, it is unable to fully match the performance of the previous MM model for the electronic DOF.

4. SUMMARY AND CONCLUSION

The purpose of this paper has been to point out that the harmonic oscillator model used by Meyer and Miller to represent the electronic DOF for a finite set of electronic states is not unique, and to consider another possibility, where each electronic state is represented as a spin- $1/2$ DOF. This spin-mapping (SM) model in some ways seems more natural than the Meyer–Miller (MM) oscillator model, since the occupation of each electronic DOF is mapped to a DOF having only two states. It is very similar to the MM model, but it is not identical to it. Application of this SM model (implemented via the SQC quantization procedure) to a standard suite of benchmark test problems has shown that it typically gives results very similar to those of the MM model oscillator model but that in no case did it completely match the MM model’s performance. It is of course possible that there may be other systems, models, parameter regimes, etc., for which the SM model does outperform the MM model.

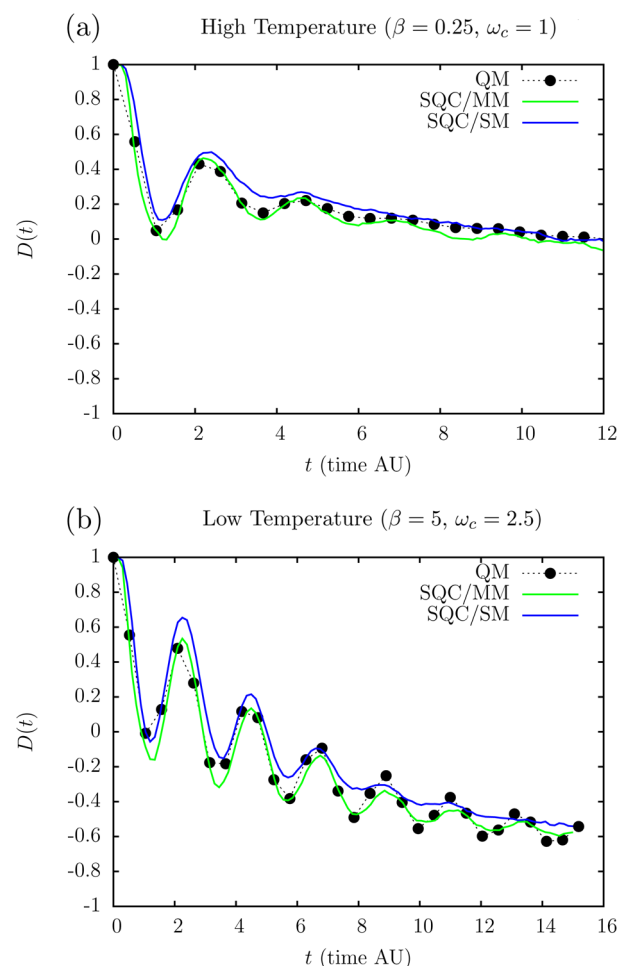


Figure 4. Asymmetric spin-Boson problem ($\epsilon = 1$, $\alpha = 0.1$, $\Delta = 1$).

One wonders whether or not there is any underlying reason why the MM model seems slightly superior performance-wise to the SM model for the electronic DOF; probably not. As noted above, they are both exact (and thus equivalent) if the vibronic Hamiltonians for each are implemented quantum mechanically; they differ, though, in their classical limits. The attractive feature of the SM model is that each electronic DOF has only two states (occupied/spin-up or unoccupied/spin-down), while the MM model’s harmonic oscillator for each electronic DOF has many states (though only two play a role in the vibronic model). The MM model, however, does likely benefit from the fact that classical harmonic oscillators often exhibit anomalously good agreement with their quantum mechanical counterparts. Ultimately, one must bear in mind that both classical models for the electronic DOF are indeed “models”, i.e., approximations, and it will therefore require more experience to see if one is typically more useful than the other.

■ A BRIEF REVIEW OF THE SQC APPROACH

As done in papers II and III, to model a non-adiabatic transition from an initial electronic state $|i\rangle$ to a final electronic state $|f\rangle$ in a system of F electronic states, we symmetrically “quantize” the initial and final “electronic” action variables representing the occupations of the states in both the MM and SM Hamiltonians. This is done by applying to the actions, $\{n_k\}$ (note $n_k = m_k + 1/2 = S_{z,k} + 1/2$ for the SM model), a joint

windowing function corresponding to the full electronic configuration associated with electronic state $|k\rangle$ given by

$$W_k(\mathbf{n}) = w_1(n_k) \prod_{k'=1, k' \neq k}^F w_0(n_{k'}) \quad (23)$$

where each $w_{N_k}(n_k)$ in eq 23 windows a single electronic DOF. In all calculations, these are chosen to be histogram “boxes”

$$w_{N_k}(n_k) = \frac{1}{2\gamma} h(\gamma - |n_k - N_k|) \quad (24)$$

whose widths are set by the ZPE γ -parameter, centered at the integer (quantum) values of the occupations N_k

$$N_k = \begin{cases} 1 & \text{for } |k\rangle \text{ occupied} \\ 0 & \text{for } |k\rangle \text{ unoccupied} \end{cases} \quad (25)$$

($h(x)$ in eq 24 is the usual Heaviside function.) Thus, γ gives the allowed deviation from the quantum values: $n_k \in [N_k - \gamma, N_k + \gamma]$. For $F = 2$ electronic states, the joint windowing function (eq 23) is thus just

$$W_k(n_1, n_2) = \begin{cases} w_1(n_1) \cdot w_0(n_2) & \text{for } |k\rangle = 1 \\ w_0(n_1) \cdot w_1(n_2) & \text{for } |k\rangle = 2 \end{cases} \quad (26)$$

To calculate a transition probability, $|f\rangle \leftarrow |i\rangle$, one evaluates by Monte Carlo

$$\tilde{P}_{f \leftarrow i}(t) = \frac{1}{(2\pi\hbar)^{G+F}} \int d\mathbf{P}_0 d\mathbf{R}_0 d\mathbf{n}_0 d\mathbf{q}_0 \times \rho(\mathbf{P}_0, \mathbf{R}_0) \cdot W_f(\mathbf{n}(t)) \cdot W_i(\mathbf{n}_0) \quad (27)$$

where $\rho(\mathbf{P}, \mathbf{R})$ is the sampling function for the G nuclear DOF and $W_i(\mathbf{n})$ is used as the sampling function for the F electronic DOF. $W_f(\mathbf{n})$ is then used to collect/bin the final time-evolved actions, $\mathbf{n}(t)$. It is essential to then renormalize these results:

$$P_{f \leftarrow i}(t) = \frac{\tilde{P}_{f \leftarrow i}(t)}{\sum_{k=1}^F \tilde{P}_{k \leftarrow i}(t)} \quad (28)$$

AUTHOR INFORMATION

Corresponding Author

*E-mail: millerwh@berkeley.edu.

Notes

The authors declare no competing financial interest.

ACKNOWLEDGMENTS

This work was supported by the National Science Foundation under Grant No. CHE-1148645 and by the Director, Office of Science, Office of Basic Energy Sciences, Chemical Sciences, Geosciences, and Biosciences Division, U.S. Department of Energy, under Contract No. DE-AC02-05CH11231. In addition, this research utilized computation resources provided by the National Energy Research Scientific Computing Center (NERSC), which is supported by the Office of Science of the U.S. Department of Energy under Contract No. DE-AC02-05CH11231. We thank Professor Michael Thoss for providing the QM results used in Figure 4.

REFERENCES

- (1) Cotton, S. J.; Miller, W. H. Symmetrical windowing for quantum states in quasi-classical trajectory simulations. *J. Phys. Chem. A* **2013**, *117*, 7190–7194.
- (2) Cotton, S. J.; Miller, W. H. Symmetrical windowing for quantum states in quasi-classical trajectory simulations: Application to electronically non-adiabatic processes. *J. Chem. Phys.* **2013**, *139*, 234112.
- (3) Cotton, S. J.; Igumenshchev, K.; Miller, W. H. Symmetrical windowing for quantum states in quasi-classical trajectory simulations: Application to electron transfer. *J. Chem. Phys.* **2014**, *141*, 084104.
- (4) Miller, W. H.; Cotton, S. J. Communication: Note on detailed balance in symmetrical quasi-classical models for electronically non-adiabatic dynamics. *J. Chem. Phys.* **2015**, *142*, 131103.
- (5) Meyer, H.-D.; Miller, W. H. A classical analog for electronic degrees of freedom in nonadiabatic collision processes. *J. Chem. Phys.* **1979**, *70*, 3214–3223.
- (6) Marcus, R. A. On the theory of oxidation-reduction reactions involving electron transfer. I. *J. Chem. Phys.* **1956**, *24*, 966–978.
- (7) Miller, W. H. Classical S matrix: numerical application to inelastic collisions. *J. Chem. Phys.* **1970**, *53*, 3578–3587.
- (8) Karplus, M.; Porter, R. N.; Sharma, R. D. Exchange reactions with activation energy. I. Simple barrier potential for (H, H₂). *J. Chem. Phys.* **1965**, *43*, 3259–3287.
- (9) Miller, W. H.; Raczkowski, A. W. Partial averaging in classical S-matrix theory. Vibrational excitation of H₂ by He. *Faraday Discuss. Chem. Soc.* **1973**, *55*, 45–50.
- (10) Bonnet, L.; Rayez, J. C. Quasiclassical trajectory method for molecular scattering processes: Necessity of a weighted binning approach. *Chem. Phys. Lett.* **1997**, *277*, 183–190.
- (11) Stock, G.; Müller, U. Flow of zero-point energy and exploration of phase space in classical simulations of quantum relaxation dynamics. *J. Chem. Phys.* **1999**, *111*, 65–76.
- (12) Müller, U.; Stock, G. Flow of zero-point energy and exploration of phase space in classical simulations of quantum relaxation dynamics. II Application to nonadiabatic processes. *J. Chem. Phys.* **1999**, *111*, 77–88.
- (13) Miller, W. H. The semiclassical initial value representation: A potentially practical way for adding quantum effects to classical molecular dynamics simulations. *J. Phys. Chem. A* **2001**, *105*, 2942–2955.
- (14) Miller, W. H. Electronically nonadiabatic dynamics via semiclassical initial value methods. *J. Phys. Chem. A* **2009**, *113*, 1405–1415.
- (15) Miller, W. H.; White, K. A. Classical models for electronic degrees of freedom: The second-quantized many-electron Hamiltonian. *J. Chem. Phys.* **1986**, *84*, 5059–5066.
- (16) Stock, G.; Thoss, M. Semiclassical description of nonadiabatic quantum dynamics. *Phys. Rev. Lett.* **1997**, *78*, 578–581.
- (17) Meyer, H.-D.; Miller, W. H. Classical models for electronic degrees of freedom: Derivation via spin analogy and application to F* + H₂ → F + H₂. *J. Chem. Phys.* **1979**, *71*, 2156–2169.
- (18) See, for example, ref 2, eqs 5–9.
- (19) Tully, J. C. Molecular dynamics with electronic transitions. *J. Chem. Phys.* **1990**, *93*, 1061–1071.
- (20) Makarov, D. E.; Makri, N. Path integrals for dissipative systems by tensor multiplication. Condensed phase quantum dynamics for arbitrarily long time. *Chem. Phys. Lett.* **1994**, *221*, 482–491.
- (21) Wang, H.; Thoss, M.; Miller, W. H. Systematic convergence in the dynamical hybrid approach for complex systems: A numerically exact methodology. *J. Chem. Phys.* **2001**, *115*, 2979–2990.